192901: mafic granulite, Aylmore Road

(Youanmi Terrane, Yilgarn Craton)

Blereau, ER, Korhonen, FJ and Kelsey, DE

Location and sampling

Hyden (SI 50-4), Pederah (2632)

MGA Zone 50, 675708E 6393163N

Warox Site FJKBGD192901

Sampled on 20 May 2009

This sample was collected from a pile of rocks in a field, about 21 km east of Powder Puff Hill, 15.1 km south of Hyden and 2.5 km southwest of the intersection of Pederah Road with Aylmore Road. The sample was collected as part of the Geological Survey of Western Australia's (GSWA) 2003–14 Yilgarn Craton Metamorphic Project, and referred to in that study as sample BG09-149. The results from this project have not been released by GSWA, although select data have been published in Goscombe et al. (2019). This sample is not available in the GSWA collections; all observations are based on descriptions presented in Goscombe et al. (2015) and have not been directly verified.

Geological context

The unit sampled is a mafic granulite of the western Youanmi Terrane of the southwest Yilgarn Craton (Quentin de Gromard et al., 2021). This unit is part of a belt of Archean metasedimentary and gneissic rocks previously assigned to the South West Terrane and referred to informally by Wilde and Pidgeon (1987) as the Wheat Belt region (cf. Wilde, 2001). However, a recent reinterpretation places the boundary between the South West and the Youanmi Terranes farther to the southwest than shown on older maps (Quentin de Gromard et al., 2021). The Youanmi Terrane contains both granite–greenstone and high-grade gneiss components with emplacement ages from c. 3010 to 2600 Ma (Quentin de Gromard et al., 2021; Cassidy et al., 2006). Existing geochronological data from this part of the Youanmi Terrane is sparse. Samples collected from Griffins Find about 74 km to the southwest yielded a range of ages. Two samples of garnet-bearing alkali feldspar granite yielded crystallization ages of c. 2636 Ma (Qiu and McNaughton, 1999). A quartzite yielded detrital zircon dates between c. 3812 and 2643 Ma, and a conservative maximum age of deposition of 2655 ± 11 Ma (GSWA 198580, Lu et al., 2015b). A pelitic gneiss yielded detrital zircon dates between c. 2838 and 2629 Ma, and a conservative maximum depositional age of 2638 ± 2 Ma (GSWA 198578, Lu et al., 2015a). Monazite from another pelitic gneiss samples yielded a weighted mean $^{207}Pb/^{206}Pb$ date of 2641 ± 6 Ma, interpreted as the age of high-grade metamorphism (GSWA 198585, Fielding et al., 2021). A summary of the metamorphic evolution of the southwest Yilgarn Craton is provided in Korhonen et al. (2021).

Petrographic description

There is limited information about this sample. It is described as a massive, medium- to coarse-grained amphibolite consisting of orthopyroxene, clinopyroxene, plagioclase, green–brown hornblende and minor ilmenite (Fig. 1). The presence of leucosomes is not described. The matrix has a polygonal granoblastic texture with equigranular grain size and straight grain margins (Fig. 1). There is no foliation or alignment of grain shapes, with a possible metamorphosed and recrystallized igneous texture preserved. Clinopyroxene is zoned, with Al-bearing augite cores and diopside rims. Mineral compositions are provided in Table 1 (Goscombe et al., 2015).

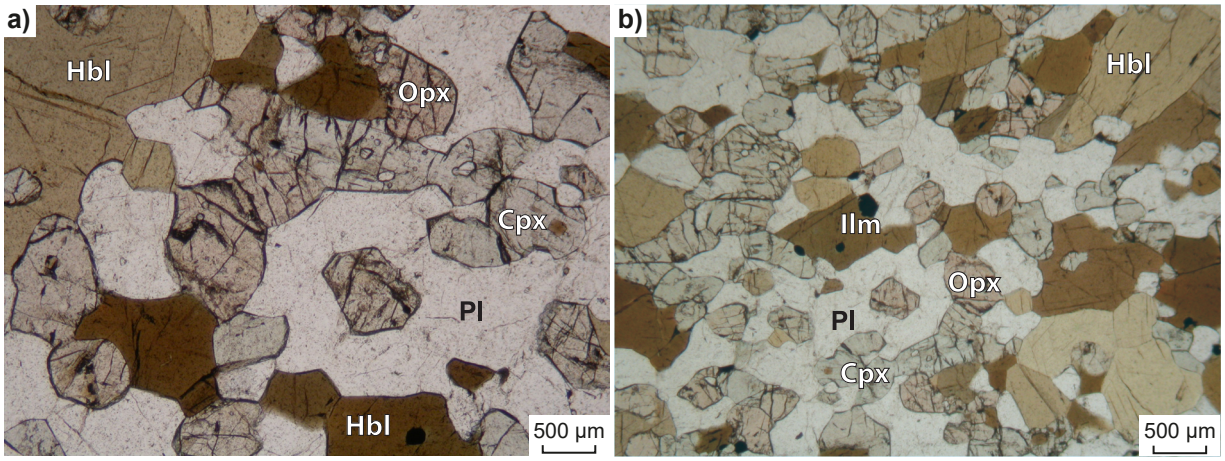

Figure 1. **Photomicrographs of sample 192901: mafic granulite, Aylmore Road, in plane-polarized light. Mineral abbreviations are explained in the caption to Figure 2**

Table 1. Mineral compositions for sample 192901: mafic granulite, Aylmore Road

Mineral[(a)]	*Hbl*	*Hbl*	*Cpx*	*Cpx*	*Pl*	*Pl*	*Ilm*	*Opx*	*Opx*
Setting	*Core*	*Rim*	*Core*	*Rim*	*Core*	*Rim*	*Core*	*Core*	*Rim*
wt%									
SiO_2	43.16	43.37	51.56	51.92	49.61	49.81	0.08	51.45	51.52
TiO_2	2.07	1.99	0.29	0.24	0.00	0.00	50.46	0.09	0.14
Al_2O_3	10.12	9.72	1.71	1.28	31.33	31.48	0.00	0.81	0.75
Cr_2O_3	0.00	0.00	0.00	0.00	0.00	0.00	0.00	0.00	0.00
FeO	14.46	14.45	9.67	9.49	0.12	0.30	46.91	26.33	26.41
MnO	0.13	0.12	0.16	0.22	0.00	0.00	1.15	0.56	0.52
MgO	12.35	12.44	13.17	13.85	0.01	0.01	0.09	19.68	19.31
ZnO	0.02	0.00	0.00	0.00	0.00	0.05	0.17	0.05	0.10
CaO	11.27	11.31	22.21	22.17	15.19	15.14	0.01	0.58	0.73
Na_2O	2.06	1.80	0.31	0.32	2.98	2.89	0.01	0.00	0.00
K_2O	0.52	0.46	0.00	0.02	0.03	0.05	0.00	0.00	0.00
Total[(b)]	96.16	95.65	99.09	99.51	99.27	99.72	98.88	99.53	99.48
Oxygen	23	23	6	6	8	8	3	6	6
Si	6.39	6.45	1.94	1.94	2.28	2.28	0.00	1.96	1.97
Ti	0.23	0.22	0.01	0.01	0.00	0.00	0.97	0.00	0.00
Al	1.77	1.70	0.08	0.06	1.70	1.70	0.00	0.04	0.03
Cr	0.00	0.00	0.00	0.00	0.00	0.00	0.00	0.00	0.00
Fe^{3+}[(c)]	0.87	0.86	0.04	0.06	0.00	0.00	0.06	0.04	0.02
Fe^{2+}	0.92	0.94	0.26	0.23	0.00	0.01	0.94	0.80	0.82
Mn^{2+}	0.02	0.01	0.01	0.01	0.00	0.00	0.02	0.02	0.02
Mg	2.73	2.76	0.74	0.77	0.00	0.00	0.00	1.12	1.10
Zn	0.00	0.00	0.00	0.00	0.00	0.00	0.00	0.00	0.00
Ca	1.79	1.80	0.90	0.89	0.75	0.74	0.00	0.02	0.03
Na	0.59	0.52	0.02	0.02	0.27	0.26	0.00	0.00	0.00
K	0.10	0.09	0.00	0.00	0.00	0.00	0.00	0.00	0.00
OH-	2.00	2.00	–	–	–	–	–	–	–
Total	15.40	15.35	4.00	4.00	5.00	5.00	2.00	4.00	4.00

NOTES: – not applicable
(a) Mineral abbreviations explained in the caption to Figure 2
(b) Totals on anhydrous basis
(c) Fe^{3+} contents based on Droop (1987)

Analytical details

Preliminary *P–T* estimates were obtained using multiple-reaction thermobarometry calculated from the mineral compositions (Table 1; Goscombe et al., 2019). These estimates were derived from the 'averagePT' module (avPT) in the program THERMOCALC version tc325 (Powell and Holland, 1988), using the internally consistent Holland and Powell (1998) dataset.

The metamorphic evolution of this sample has subsequently been re-evaluated using phase equilibria modelling, based on the bulk-rock composition (Table 2). The bulk-rock composition was determined by X-ray fluorescence spectroscopy, together with loss on ignition (LOI). The modelled O content (for Fe^{3+}) was set to be 20% of the measured total Fe; the modelled H_2O content was the measured LOI. The bulk composition was also adjusted for the presence of apatite by applying a correction to CaO (Table 2). Thermodynamic calculations were performed in the NCKFMASHTO (Na_2O–CaO–K_2O–FeO–MgO–Al_2O_3–SiO_2–H_2O–TiO_2–O) system using THERMOCALC version tc340 (updated October 2013; Powell and Holland, 1988) and the internally consistent thermodynamic dataset of Green et al. (2016; version dataset tc-ds63, created January 2015). The activity–composition relations used in the modelling are detailed in Green et al. (2016); the augite model was used for clinopyroxene. Additional information on the workflow with relevant background and methodology is provided in Korhonen et al. (2020).

Table 2. Measured whole-rock and modelled compositions for sample 192901: mafic granulite, Aylmore Road

XRF whole-rock composition (wt%)												
SiO_2	**TiO_2**	**Al_2O_3**	**Fe_2O_3**	**FeO[a]**	**MnO**	**MgO**	**CaO**	**Na_2O**	**K_2O**	**P_2O_5**	**LOI**	**Total**
46.80	0.84	15.00	–	12.87	0.20	9.47	10.90	1.53	0.17	0.09	0.12	97.99
Normalized composition used for phase equilibria modelling (mol%)												
SiO_2	**TiO_2**	**Al_2O_3**	**O[b]**	**FeO^{T}[c]**	**MnO**	**MgO**	**CaO[d]**	**Na_2O**	**K_2O**	**–**	**H_2O[e]**	**Total**
49.48	0.67	9.35	1.02	10.24	–	14.93	12.21	1.57	0.11	–	0.42	100

NOTES: (a) FeO content is total Fe
(b) O content (for Fe_2O_3) set to be 20% of measured FeO[b]
(c) FeO^T = moles FeO + 2 * moles O
(d) CaO modified to remove apatite: CaO(Mod) = CaO(Total) - (moles CaO(in Ap) = 3.33 * moles P_2O_5)
(e) H_2O content is the measured LOI
– not applicable

Results

The *P–T* pseudosection for this sample was calculated over a *P–T* range of 2–10 kbar and 700–1000 °C (Fig. 2). The solidus is located between 905 and 970 °C across the modelled range of pressures. Magnetite is stable below 6.6 kbar at 815 °C, and rutile is stable above 7.3 kbar at 700 °C. Garnet has a minimum pressure stability of 5.5 kbar at 700 °C, and increases with increasing temperature. Biotite has a maximum temperature stability of 910 °C at 2.5 kbar, which decreases with increasing pressure. Quartz is stable above 6.9 kbar at 700 °C and above 10 kbar at 940 °C.

Metamorphic *P–T* estimates (± 2σ uncertainty) calculated using multiple-reaction thermobarometry are 4.6 ± 1.1 kbar and 771 ± 27 °C (Goscombe et al., 2019). These calculations used mineral core compositions (Table 1) to estimate peak conditions. Conventional thermobarometry using the orthopyroxene–clinopyroxene and hornblende–clinopyroxene thermometers reportedly yield similar temperatures of 750–795 °C, and the Al-in-hornblende barometer yields 5.1 ± 0.5 kbar (Goscombe et al., 2019).

Interpretation

Based on the limited information available, the peak metamorphic assemblage is interpreted to be hornblende–orthopyroxene–clinopyroxene–plagioclase–ilmenite. This assemblage field is stable between 815 and 965 °C at 5.4 – 8.8 kbar. The peak field is delimited by the stability of garnet at higher pressures, the solidus at higher temperatures and the stability of magnetite at lower pressures. The modelling predicts up to 1.5% magnetite (molar proportions approximately equivalent to vol%) in the hornblende–orthopyroxene–clinopyroxene–plagioclase–ilmenite–magnetite field at lower pressure. The petrographic description includes ilmenite but not magnetite; therefore, magnetite is inferred not to be present in the

sample. However, the stability of magnetite is sensitive to the O content used in the modelling, which is not well constrained. As such, there is uncertainty on the lower-pressure bound on the interpreted peak assemblage field. There is also no information on whether the sample may have contained partial melt, which would extend the peak field to higher temperature.

Multiple-reaction and conventional thermobarometry yield slightly lower *P–T* estimates than the results derived from phase equilibria modelling. There is no information on the prograde and retrograde segments of the *P–T* path, and therefore the overall shape of the *P–T* path is not defined.

Based on the results of phase equilibria modelling, peak metamorphic conditions are estimated at 815–965 °C and 5.4 – 8.8 kbar, defining an apparent thermal gradient between 110 and 180 °C/kbar.

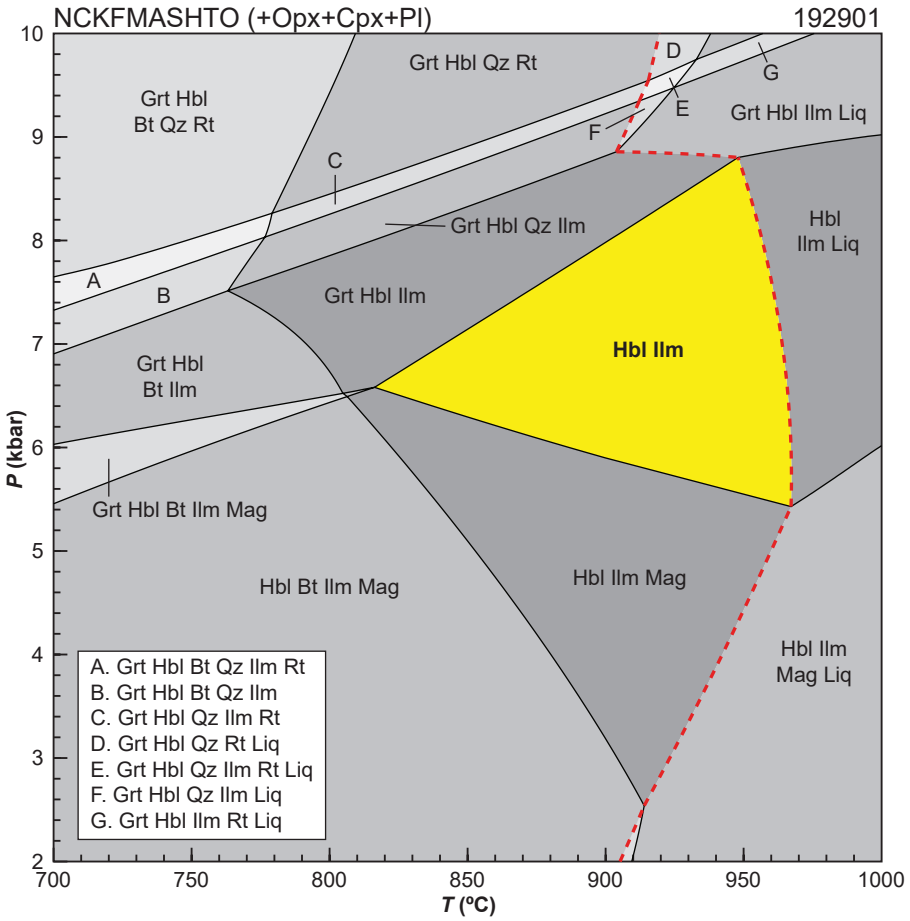

Figure 2. ***P–T* pseudosection calculated for sample 192901: mafic granulite, Aylmore Road. Assemblage field corresponding to peak metamorphic conditions is shown in bold text and yellow shading. Red dashed line represents the solidus. Abbreviations: Bt, biotite; Cpx, clinopyroxene; Grt, garnet; Hbl, hornblende; Ilm, ilmenite; Liq, silicate melt; Opx, orthopyroxene; Pl, plagioclase; Qz, quartz; Rt, rutile**

References

Cassidy, KF, Champion, DC, Krapež, B, Barley, ME, Brown, SJA, Blewett, RS, Groenewald, PB and Tyler, IM 2006, A revised geological framework for the Yilgarn Craton, Western Australia: Geological Survey of Western Australia, Record 2006/8, 8p.

Droop, GTR 1987, A general equation for estimating Fe^{3+} concentrations in ferromagnesian silicates and oxides from microprobe analyses, using stoichiometric criteria: Mineralogical Magazine, v. 51, no. 361, p. 431–435.

Fielding, IOH, Wingate, MTD, Korhonen, FJ and Rankenburg, K 2021, 198585: pelitic gneiss, Griffins Find; Geochronology Record 1767: Geological Survey of Western Australia, 5p.

Goscombe, B, Blewett, R, Groenewald, PB, Foster, D, Wade, B, Wyche, S, Wingate, MTD and Kirkland, CL 2015, Metamorphic Evolution of the Yilgarn Craton: Geological Survey of Western Australia (unpublished), 910p.

Goscombe, B, Foster, DA, Blewett, R, Czarnota, K, Wade, B, Groenewald, B and Gray, D 2019, Neoarchaean metamorphic evolution of the Yilgarn Craton: a record of subduction, accretion, extension and lithospheric delamination: Precambrian Research, v. 335, article no. 105441, doi:10.1016/j.precamres.2019.105441.

Green, ECR, White, RW, Diener, JFA, Powell, R, Holland, TJB and Palin, RM 2016, Activity–composition relations for the calculation of partial melting equilibria in metabasic rocks: Journal of Metamorphic Geology, v. 34, no. 9, p. 845–869.

Holland, TJB and Powell, R 1998, An internally consistent thermodynamic data set for phases of petrological interest: Journal of Metamorphic Geology, v. 16, no. 3, p. 309–343.

Korhonen, FJ, Blereau, ER, Kelsey, DE, Fielding, IOH and Romano, SS 2021, Metamorphic evolution of the southwest Yilgarn, *in* Accelerated Geoscience Program extended abstracts: Geological Survey of Western Australia, Record 2021/4, p. 108–115.

Korhonen, FJ, Kelsey, DE, Fielding IOH and Romano, SS 2020, The utility of the metamorphic rock record: constraining the pressure–temperature–time conditions of metamorphism: Geological Survey of Western Australia, Record 2020/14, 24p.

Lu, Y, Wingate, MTD, Kirkland, CL, Goscombe, B and Wyche, S 2015a, 198578: pelitic gneiss, Griffins Find; Geochronology Record 1284: Geological Survey of Western Australia, 4p.

Lu, Y, Wingate, MTD, Kirkland, CL, Goscombe, B and Wyche, S 2015b, 198580: quartzite, Griffins Find; Geochronology Record 1285: Geological Survey of Western Australia, 5p.

Powell, R and Holland, TJB 1988, An internally consistent dataset with uncertainties and correlations: 3. Applications to geobarometry, worked examples and a computer program: Journal of Metamorphic Geology, v. 6, no. 2, p. 173–204.

Qiu, Y and McNaughton, NJ 1999, Source of Pb in orogenic lode-gold mineralisation: Pb isotope constraints from deep crustal rocks from the southwestern Archaean Yilgarn Craton, Australia: Mineralium Deposita, v. 34, p. 366–381.

Quentin de Gromard, R, Ivanic, TJ and Zibra, I 2021, Pre-Mesozoic interpreted bedrock geology of the southwest Yilgarn, 2021, *in* Accelerated Geoscience Program extended abstracts: Geological Survey of Western Australia, Record 2021/4, p. 122–144.

Wilde, SA 2001, Jimperding and Chittering metamorphic belts, Western Australia— a field guide: Geological Survey of Western Australia, Record 2001/12, 24p.

Wilde, SA and Pidgeon, RT 1987, U–Pb geochronology, geothermometry and petrology of the main areas of gold mineralization in the 'Wheat Belt' region of Western Australia: Western Australian Minerals and Petroleum Research Institute, Project 30, Final Report, 171p

Links

Metamorphic history introduction document: Intro_2020.pdf

Recommended reference for this publication

Blereau, ER, Korhonen, FJ and Kelsey, DE 2022, 192901: mafic granulite, Aylmore Road; Metamorphic History Record 12: Geological Survey of Western Australia, 6p.

Data obtained: 28 July 2020

Date released: 14 April 2022

This Metamorphic History Record was last modified on 29 March 2022.

Grid references in this publication refer to the Geocentric Datum of Australia 1994 (GDA94). All locations are quoted to at least the nearest 100 m.

WAROX is GSWA's field observation and sample database. WAROX site IDs have the format 'ABCXXXnnnnnnSS', where ABC = geologist username, XXX = project or map code, nnnnnn = 6 digit site number, and SS = optional alphabetic suffix (maximum 2 characters).

Isotope and element analyses are routinely conducted using the GeoHistory laser ablation ICP-MS and Sensitive High-Resolution Ion Microprobe (SHRIMP) ion microprobe facilities at the John de Laeter Centre (JdLC), Curtin University, with the financial support of the Australian Research Council and AuScope National Collaborative Research Infrastructure Strategy (NCRIS). The TESCAN Integrated Mineral Analyser (TIMA) instrument was funded by a grant from the Australian Research Council (LE140100150) and is operated by the JdLC with the support of the Geological Survey of Western Australia, The University of Western Australia (UWA) and Murdoch University. Mineral analyses are routinely obtained using the electron probe microanalyser (EPMA) facilities at the Centre for Microscopy, Characterisation and Analysis at UWA, and at Adelaide Microscopy, University of Adelaide.

Digital data related to WA Geology Online, including geochronology and digital geology, are available online at the Department's Data and Software Centre and may be viewed in map context at GeoVIEW.WA.

Disclaimer

This product uses information from various sources. The Department of Mines, Industry Regulation and Safety (DMIRS) and the State cannot guarantee the accuracy, currency or completeness of the information. Neither the department nor the State of Western Australia nor any employee or agent of the department shall be responsible or liable for any loss, damage or injury arising from the use of or reliance on any information, data or advice (including incomplete, out of date, incorrect, inaccurate or misleading information, data or advice) expressed or implied in, or coming from, this publication or incorporated into it by reference, by any person whosoever.

Further details of geoscience products are available from:

Information Centre
Department of Mines, Industry Regulation and Safety
100 Plain Street
EAST PERTH WA 6004
Telephone: +61 8 9222 3459 | Email: publications@dmirs.wa.gov.au
www.dmirs.wa.gov.au/GSWApublications